Eur. Phys. J. B **41**, 281–287 (2004)
DOI: 10.1140/epjb/e2004-00318-3

THE EUROPEAN PHYSICAL JOURNAL B

A potential model for single crystals of the Li_2O-B_2O_3 system based on non-equivalence of boron atoms

V.V. Maslyuk[1,a], T. Bredow[2], and H. Pfnür[1]

[1] Institut für Festkörperphysik, Universität Hannover, Appelstr. 2, 30167 Hannover, Germany
[2] Theoretische Chemie, Universität Hannover, Am Kleinen Felde 30, 30167 Hannover, Germany

Received 27 May 2004 / Received in final form 14 July 2004
Published online 21 October 2004 –

Abstract. Ab initio calculations allow to distinguish boron atoms in BO_3 and BO_4 complexes in lithium borates. On this basis an effective potential model for single crystals of Li_2O-B_2O_3 is suggested. Empirical parameters of the interaction potentials are optimized in order to reproduce the experimental data of lithium tetraborate. The optimized parameters are applied to calculations of the structures of the anhydrous borate single crystals Li_3BO_3, $LiBO_2$, $Li_2B_4O_7$, $Li_3B_7O_{12}$ and LiB_3O_5. The range of applicability of the potential model is increased by introducing a dependence of the effective oxygen charges on the Li content. In this way good agreement with experimental data is obtained for calculated structural and elastic properties.

PACS. 61.50.Ah Theory of crystal structure, crystal symmetry; calculations and modeling – 34.20.Cf Interatomic potentials and forces – 12.39.Pn Potential models – 77.84.Bw Elements, oxides, nitrides, borides, carbides, chalcogenides, etc.

1 Introduction

The Li_2O-B_2O_3 system is attractive for theorists and experimentalists not only because of its interesting properties, but also because of its perspectives for practical applications. According to the general Li_2O-B_2O_3 phase diagram based on available literature data [1–3], 8 stoichiometric compounds exist in this system. Only 5 of these are stable at room temperature, namely Li_3BO_3 (lithium orthoborate), $Li_6B_4O_9$ and $LiBO_2$ (lithium metaborates), $Li_2B_4O_7$ (lithium tetraborate) and LiB_3O_5 (lithium triborate). The two latter compounds are promising for practical applications. LiB_3O_5 single crystals are suitable for the 2nd and 3rd YAG:Nd laser harmonic generation [4–6], the development of parametric light generators [7,8] and as wave-guides [9]. $Li_2B_4O_7$ single crystals can be used as substrates for thermostable surface [10–12] and bulk [13] acoustic wave-based devices, as pyroelectric temperature sensors [14], as non-linear optical device for the 4th and 5th YAG:Nd single crystal laser harmonics generation [15] and for thermoluminescent dosimetry of X-ray, gamma and neutron radiation [16–18].

Other crystals (Li_3BO_3, $Li_6B_4O_9$, $LiBO_2$) have been studied less frequently and their only known properties are the superionicity in Li_3BO_3 [19] and the layering of the $LiBO_2$ system [20].

A common feature of all anhydrous lithium borate crystalline structures is the boron-oxygen anion subsystem. It is capable of producing a covalent three-dimensional framework based on two stable oxygen coordinations of boron atoms – BO_3-triangles and BO_4-tetrahedrons. Lithium atoms, in turn, are connected with the anion subsystem by electrostatic interaction. The most interesting crystalline structure has been found in the $Li_2B_4O_7$ crystal. The anion sublattice is formed by double helices in the [001] direction with lithium ions in their channels. The double helices are created by $(B_4O_9)^{6-}$-anions consisting of two BO_3 and two BO_4 units.

The large number of studies of compounds in the Li_2O-B_2O_3 system available in the literature allows to use a systematic approach to describe their physical properties. The complexity of the crystals structures of the Li_2O-B_2O_3 systems (from 16 to 104 atoms in unit cell) does not allow ab initio calculations to be applied especially for dynamic properties investigations. Therefore the adequate approach is to use the classical methods based on interatomic interaction potentials. Several molecular dynamics studies [21–28] of the borate compounds have been published. In reference [22] the borate glasses were investigated, but only BO_3 was used as main element of possible structures. A classical potential model based on Buckingham potentials and on three-body harmonic interaction potentials of O-B-O angles in BO_3 and BO_4 was

[a] e-mail: maslyuk@fkp.uni-hannover.de

applied to lithium borate glasses [24–27]. We have tested this model for single crystals of the Li_2O-B_2O_3 system and obtained poor agreement for the lattice parameters. This motivated us to attempt a systematical improvement of effective potentials for the description of this system.

In this paper, a potential model is suggested for the description of the structures of a number of crystals in the Li_2O-B_2O_3 system. The model takes into account the non-equivalence of the boron atoms in the structural complexes BO_3 and BO_4. The investigation of the boron-oxygen subsystem has been performed by using ab initio calculations of BO_3, BO_4 complexes. Such type of investigation allows to predict some features which are common for all anhydrous borates, but have not yet been studied experimentally. The parameters of the classical interatomic potentials were fitted to experimental data of $Li_2B_4O_7$ with the GULP program [29].

As we will show, the parameters derived by this procedure are fairly general and can be directly used to describe the crystal structures of related compounds. Explicit tests, which have been performed for α-B_2O_3 [30], β-B_2O_3 [31], Li_3BO_3 [32], $LiBO_2$ [33], $Li_2B_4O_7$ [34], LiB_3O_5 [35] and $Li_3B_7O_{12}$ [36] (exists at high temperatures), are presented here. A characteristic feature of our modelling approach is the use of adjustable effective charges for the atoms. This makes the model more flexible to describe structures of different compositions. The effective charges obtained during the fitting procedure to lithium borate crystal structures and values of acoustic modes at the Γ-point show an almost linear dependence on the mole fraction of Li_2O.

Based on the analysis of hybridization in the BO_3 and BO_4 building units, we came to the conclusion that the interaction of the atoms of the two units must be described with different sets of parameters. This scheme can be generalized to other compounds that contain atoms in different hybridizations.

Accurate and reliable interatomic potentials for lithium borate solids enable to apply molecular dynamics methods in theoretical investigations of the temperature dependence of their structural parameters. The suggested approach allows to extend the potential model to other anhydrous borates and to determine a variety of properties.

2 Potential model

Our potential model is based on two-particle and three-particle potentials as in previous approaches, e.g. in reference [24]. For the description of two-particle interactions we have chosen the Buckingham potential [29]:

$$U_{ij} = b_{ij} \exp\left(-\frac{r_{ij}}{\rho_{ij}}\right) + \frac{q_i q_j e^2}{r_{ij}} \qquad (1)$$

where the individual terms represent the Born-Mayer repulsion and the Coulomb potential, respectively. Here, r_{ij} is the interatomic distance between ions i and j, e is the elementary charge, q_i is the effective charge of the ion i and b_{ij}, ρ_{ij} are the parameters of the potential model.

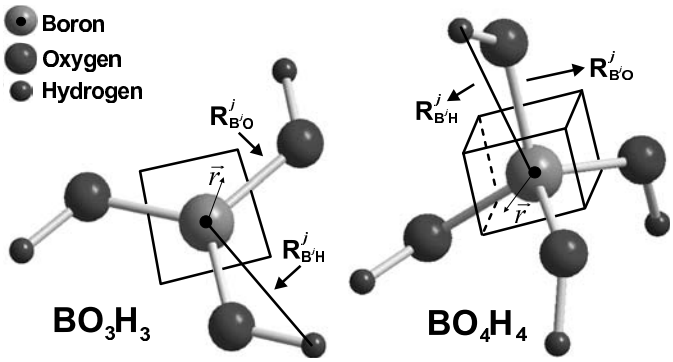

Fig. 1. BO_3H_3 and $(BO_4H_4)^{1-}$ complexes with displacement vectors $\boldsymbol{r}$, and interatomic distances R.

The electrostatic energy was calculated using the Ewald summation technique [37].

The three-particle interaction was described with a harmonic term [29]:

$$U_{ijk} = \frac{1}{2} A_{ijk} \left(\Theta_{ijk} - \Theta_0\right)^2, \qquad (2)$$

where Θ_{ijk} is the angle formed by the ions i, j, k with ion i being placed in the middle, A_{ijk} is a constant determining the strength of the angular interaction and Θ_0 is the equilibrium angle.

The optimal values of q_i, b_{ij}, ρ_{ij} and Θ_0, A_{ijk} have been obtained by fitting the model potentials to experimental data of $Li_2B_4O_7$, namely crystallographic data [34,38] (extrapolated from 80–300 K to 0 K), elastic constants [39] and the values of three acoustic modes at the Γ point.

Before deriving the parameters of the potential model we performed ab initio calculations of the BO subsystem, namely of the BO_3 and BO_4 complexes. This preliminary investigation was intended to analyze long-range and short-range B-O interactions in BO_3 and BO_4 which cannot be separated experimentally.

The parameters of the short-range B-O interaction were optimized by fitting the effective potential (2) to the quantum-chemical energy hypersurface of BO_3H_3 and $(BO_4H_4)^-$. These energies were defined using the following relation:

$$U(\boldsymbol{r}) = U_{\mathrm{BOH}}(\boldsymbol{r}) - U_{\mathrm{OH}} - U_{\mathrm{B}}. \qquad (3)$$

Here $U_{\mathrm{BOH}}(\boldsymbol{r})$, $\mathrm{U_{OH}}$ and U_{B} are the total energies of BO_nH_n complexes ($n = 3, 4$), O_nH_n groups ($n = 3, 4$) and the B^{3+} ion, respectively. $\boldsymbol{r}$ is the B ion displacement from equilibrium position in the BO_3 plane (within a quadratic region) for BO_3H_3 and in space (in a cubic region) for $(BO_4H_4)^-$ (see Fig. 1). The maximal value of boron displacement from equilibrium position was $r_{max} = 0.2$ Å. About 300 single points were calculated for each complex in the parameter fitting procedure. We neglect the B-H interaction because the B-H distances are relatively large (more than 2 Å). The quantum-chemical reference energies were calculated at Hartree-Fock level

with a 6-31G [40] basis set. The quantum-chemical package CRYSTAL03 [41] was used.

Parameters b_{ij}, ρ_{ij}, were found by a χ^2 minimizing procedure using the linearization method [42] realized in the FUMILY procedure [43] and applied to the following expression

$$\chi^2 = \sum_j \left[U(\boldsymbol{r}^j) - \left(b_{\mathrm{B}^i\mathrm{O}} \exp\left(-\frac{R^j_{\mathrm{B}^i\mathrm{O}}}{\rho_{\mathrm{B}^i\mathrm{O}}} \right) + \frac{q_{\mathrm{B}^i} q_{\mathrm{O}} e^2}{R^j_{\mathrm{B}^i\mathrm{O}}} + \frac{q_{\mathrm{B}^i} q_{\mathrm{H}} e^2}{R^j_{\mathrm{B}^i\mathrm{H}}} \right) \right]^2, \quad (4)$$

where $\boldsymbol{r}^j$ is the jth boron atom displacement from equilibrium position, q_{B^i}, q_{O}, q_{H} are the B^i, O, H ion charges, respectively. $R^j{}_{\mathrm{B}^i\mathrm{O}}$, $R^j{}_{\mathrm{B}^i\mathrm{H}}$ are the B^iO and B^iH bond length at step j. We chose the values of the effective atomic charges as $q_{\mathrm{B}^1} = q_{\mathrm{B}^2} = +3$, $q_{\mathrm{O}} = -2$ and $q_{\mathrm{H}} = +1$. Since ρ_{BO} and b_{BO} are correlated, we used the same value ρ_{BO} for both interactions B^1-O and B^2-O. For this parameter, a value of 0.28 Å was obtained. But the most important result was that the optimal value of parameter b substantially differs for the two types of boron atoms, $b_{\mathrm{B}^1\mathrm{O}} = 743.17$ eV and $b_{\mathrm{B}^2\mathrm{O}} = 863.97$ eV. In addition, a Mulliken analysis [44] of the HF wavefunction of the two models BO_3H_3 and $(BO_4H_4)^-$ shows that the charges of boron atoms are also different ($q_{\mathrm{B}^1} = +1.32$ and $q_{\mathrm{B}^2} = +1.45$). The different charges of q_{B^1} and q_{B^2} and the different parameters of the potentials for B-O interaction in BO_3 and BO_4 allow to identify B^1 and B^2 as two ions with the same mass but different charges and interactions with O atoms. This is not surprising because the complexes BO_3 (sp^2) and BO_4 (sp^3) have different types of hybridization. This result was the basis for the development of our improved potential model. The details of parameter optimization are described in the next section.

2.1 Fitting of potential model parameters

The parameters of our potential model for the $Li_2B_4O_7$ crystal were derived using a BFGS optimization procedure [45] as implemented in the GULP program [29].

The choice of the start parameter set was based on the known crystallographic data, on previous potential models and on the results of the our ab initio calculations described above. Only interactions between Li-O, O-O, B^1-O, B^2-O and O-B^1-O, O-B^2-O, B^1-O-B^2, B^1-O-B^1, B^2-O-B^2 were taken into account. We neglect short-range Li-Li, B-B and Li-B interactions because the interatomic distances are large (more than 3 Å). A cut-off radius of 10.0 Å has been applied to the two-body interactions throughout the simulations. During the fitting procedure all parameters (q_i, b_{ij}, ρ_{ij} and Θ_0, A_{ijk}) were allowed to change. The parameters of the three-particle interaction of B^1-O-B^1 triples which are absent in $Li_2B_4O_7$ were found by fitting them to the structure of α-B_2O_3.

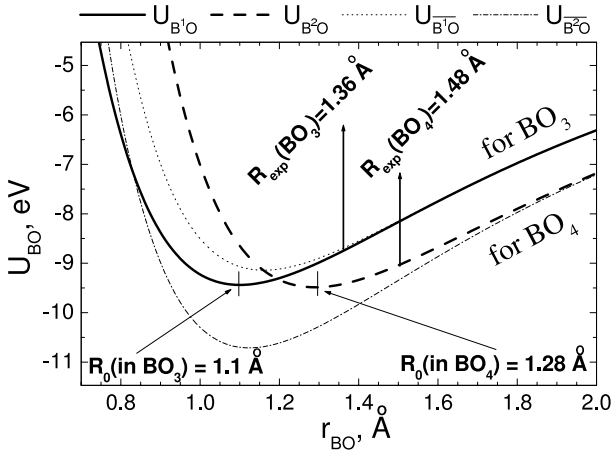

Fig. 2. Fitted and simulated U_{BO} potentials for B-O interactions in BO_3 and BO_4 units. $U_{\mathrm{B_1O}}$ and $U_{\mathrm{B_2O}}$ are the obtained potentials with different b_{ij}; $U_{\overline{\mathrm{B_1O}}}$ and $U_{\overline{\mathrm{B_2O}}}$ are the simplified potentials with the same $b_{ij} = (b_{\mathrm{B^1O}} + b_{\mathrm{B^2O}})/2$.

Table 1. Optimized values for the parameters of the classical potential model for crystals of the Li_2O-B_2O_3 system (Eqs. (1) and (2)).

Interaction	Parameters and their values	
Li-O	b_{LiO}=1426.45 eV	ρ_{LiO}=0.236 Å
O-O	$b_{\mathrm{OO}} = 141704.69$ eV	$\rho_{\mathrm{OO}} = 0.183$ Å
B^1-O	$b_{\mathrm{B^1O}} = 537.35$ eV	$\rho_{\mathrm{B^1O}} = 0.198$ Å
B^2-O	$b_{\mathrm{B^2O}} = 1164.83$ eV	$\rho_{\mathrm{B^2O}} = 0.198$ Å
O-B^1-O	$\Theta_{\mathrm{OB^1O}} = 120.07°$	$A_{\mathrm{OB^1O}} = 12.18$ eV/degree
O-B^2-O	$\Theta_{\mathrm{OB^2O}} = 109.41°$	$A_{\mathrm{OB^2O}} = 5.40$ eV/degree
B^1-O-B^2	$\Theta_{\mathrm{B^1OB^2}} = 120.67°$	$A_{\mathrm{B^1OB^2}} = 2.58$ eV/degree
B^1-O-B^1	$\Theta_{\mathrm{B^1OB^2}} = 135.41°$	$A_{\mathrm{B^1OB^2}} = 3.70$ eV/degree
B^2-O-B^2	$\Theta_{\mathrm{B^2OB^2}} = 135.68°$	$A_{\mathrm{B^2OB^2}} = 3.91$ eV/degree
Elements	$Li_2B_4O_7$ atomic charges	Derived from experiment [46]
Li	0.664	0.8 ± 0.1
B^1	1.072	$\}$ 1.23±0.05
B^2	1.223	
O	−0.846	−0.93±0.01

The final parameters of our potential model are shown in Table 1. The large value of parameter b_{OO}, 141705.69 eV, is a result of the previously mentioned correlation between b_{ij} and ρ_{ij}.

It should be noted that our model gives reasonable atomic charges ($q_{\mathrm{Li}} = +0.66$, $q_{\mathrm{B}} = +1.07$ and $+ 1.22$, $q_{\mathrm{O}} = -0.85$) which agree well with charges derived from the longitudinal optical and transverse optical splitting in Raman spectra, $q_{\mathrm{Li}} = +0.8 \pm 0.1$, $q_{\mathrm{B}} = +1.23 \pm 0.05$, $q_{\mathrm{O}} = -0.93 \pm 0.01$ (Tab. 1).

In order to demonstrate the importance of discrimination between two types of boron atoms (B^1 and B^2) we compared the optimized BO potentials (Tab. 1) with simplified potentials, where b_{BO} was set equal to the average value between $b_{\mathrm{B^1O}}$ and $b_{\mathrm{B^2O}}$. Figure 2 shows our potentials $U_{\mathrm{B_1O}}$ and $U_{\mathrm{B_2O}}$ and the simplified $U_{\overline{\mathrm{B_1O}}}$ and $U_{\overline{\mathrm{B_2O}}}$. Other parameters of (1) and atomic charges were not

changed. After analysis of the behavior of the two types of the potentials we draw the following conclusions:

- According to our potential model, the boron sp^2 (in BO_3) and sp^3 (in BO_4) hybridization leads to different types of B-O interactions. The equilibrium bonds R_0 (the bond length at the potential minimum) and the potential curvature of BO_3 (R_0 = 1.10 Å), BO_4 (R_0 = 1.29 Å) are different. The experimental bond distances R_{exp} in BO_3 and BO_4 of all crystals of Li_2O-B_2O_3 system differ from R_0 practically by the same distance (0.25 Å for BO_3 and 0.2 Å for BO_4). Note that R_0 is the distance between B (in sp^2 or sp^3 states) and O atoms for a BO molecule. The average differences between R_{exp} and calculated R_{BO} is 0.04 Å for BO_3 and 0.01 Å for BO_4. The shifting from R_0 to R_{exp} occurs via O-O interactions in the BO_3 and BO_4 units.
- The second derivatives of U_{B^1O} and U_{B^2O} at $R = R_{exp}$ are different, thus they yield different frequencies of local vibrations of the BO_3 and BO_4 units. For potentials $U_{\overline{B_1O}}$ and $U_{\overline{B_2O}}$ force constants are also different but they are in the range between the force constants of U_{B_1O} and U_{B_2O} (this can simply be obtained by differentiation of (1)).

While it is clear that for a given temperature it will always be possible to obtain a good description of the crystal structure and other properties by equating b_{B^1O} and b_{B^2O} and changing values of three-particle potentials, this simplified model will not be able to describe reasonably well the temperature evolution of the system and its properties. As result, it can not be used for molecular dynamics calculations at different temperatures. For this reason we suggest that also for other systems where sp^2 and sp^3 hybridizations of the same elements are present it will be necessary to make an additional investigation of atom interactions.

3 Application of the potential model for the prediction of the structure of Li_2O-B_2O_3 single crystals

3.1 Quality of the potential

The results of our calculations for the $Li_2B_4O_7$ structure, for the elastic constants and for the Young's modulus are presented in Table 2. A good agreement of calculated and experimental crystal structure parameters and elastic properties is obtained. This was expected because the experimental data were used during the parameter optimization. The error of lattice parameters does not exceed 0.05 Å, which is in the range of errors of ab initio calculations [47]. Our potential model also provides good agreement for the Young's modulus (Tab. 2) which was not used in the fitting procedure. Absolute errors for the Young's modulus does not exceed 7 GPa for E_{100} (E_{010}) and 38 GPa for E_{001}.

Table 2. Crystal structure and elastic properties of $Li_2B_4O_7$[a]. Lattice parameters a, c (Å), fractional coordinates x, y, z, elastic constants C (Pa), Young's modulus E (GPa).

Property	Experiment	This work (GULP)
Volume, Å^3	924.57	936.12
a, Å	9.479	9.525
c, Å	10.290	10.319
Li (x, y, z)	(0.1497, 0.1651, 0.8508)	(0.1536, 0.1686, 0.8508)
$B^1(x, y, z)$	(0.1681, 0.0861, 0.2007)	(0.1739, 0.0844, 0.2044)
$B^2(x, y, z)$	(0.9463, 0.1125, 0.0824)	(0.9459,0.1165, 0.0835)
O (x, y, z)	(0.2817, 0.1372, 0.2653)	(0.2792, 0.1284, 0.2591)
O (x, y, z)	(0.0671, 0.1776, 0.1562)	(0.0703, 0.1752, 0.1589)
O (x, y, z)	(0.1562, 0.9432, 0.1811)	(0.1560, 0.9455, 0.1836)
O (x, y, z)	(0.0000, 0.0000, 0.0000)	(0.0000, 0.0000, 0.0101)
C_{11}, 10^{10} Pa	13.53[b], 12.68[c], 13.50[d]	13.56
C_{33}, 10^{10} Pa	5.48[b], 6.82[c], 5.68[d]	5.48
C_{44}, 10^{10} Pa	5.74[b], 5.85[c], 5.85[d]	5.29
C_{66}, 10^{10} Pa	4.74[b], 4.57[c], 4.67[d]	4.34
C_{12}, 10^{10} Pa	0.11[b], 0.10[c], 0.36[d]	0.22
C_{13}, 10^{10} Pa	3.186[b], 2.39[c], 3.35[d]	2.94
E_{100}, GPa	118.7[c]	111.8
E_{010}, GPa	118.7[c]	111.8
E_{001}, GPa	58.4[c]	21.3

[a] lattice parameters [34]; [b] [39]; [c] [48]; [d] [49].

The limits of the present potential model with respect to different oxygen environments of the boron atoms were tested by molecular dynamics (MD) simulations. The calculations were performed with a NPT-ensemble in conjunction with the Nosé-Hoover [50] thermostat and the Parrinello-Rahman [51] barostat. The box simulation contained 832 atoms ($2 \times 2 \times 2$ supercell). The system was allowed to evolve for 50 ps. A time step of 1 fs was used for integrating the equation of motion.

In a previous study [47] via ab initio calculations the pressing and stretching of α-B_2O_3 (with BO_3 building unit) and β-B_2O_3 (with BO_4 building unit) was investigated. It was assumed that the first four shortest B-O distances in compressed α-B_2O_3 participate in B-O bonding when they are smaller than 2.7 Å. Our MD simulation shows that the maximum value of B^1-O (B^2-O) bonds does not exceed 2.2 Å (2.5 Å) below 900 K which is 290 K bellow the experimental melting point. Higher temperatures were not investigated.

The obtained results of bond distances show that it is possible to use the present model without taking into account changes in the BO coordination environment up to 900 K. The difference between maximal values of the B^1O and B^2O bonds during MD calculations shows that the crystal structure can be destroyed by a $BO_4 \rightarrow BO_3 + O^{2-}$ transition.

3.2 Prediction for other single crystals of the Li_2O-B_2O_3 system

The structure parameters of the other single crystals α-B_2O_3, β-B_2O_3, Li_3BO_3, $LiBO_2$, $Li_2B_4O_7$, LiB_3O_5 and $Li_3B_7O_{12}$ were optimized with the present model. The results are shown in Table 3. The effective atomic charges

Table 3. Comparison of calculated and experimental structure parameters for Li_2O-B_2O_3 system single crystals.

Crystal (symmetry)	Properties	Calc. without fitting charges	Calc. with fitting charges	Experiment
α-B_2O_3* [30]	Volume, Å^3	135.31		135.77
($P3_1$)	a, Å	4.35		4.34
	c, Å	8.26		8.34
β-B_2O_3 [31]	Volume, Å^3	148.63		163.54
($Ccm2_1$)	a, Å	4.61		4.86
	b, Å	7.80		7.88
	c, Å	4.13		4.27
LiB_3O_5[35]	Volume, Å^3	300.10	320.42	320.42
($Pna2_1$)	a, Å	8.00	8.42	8.45
	b, Å	7.15	7.43	7.38
	c, Å	5.25	5.20	5.14
$Li_3B_7O_{12}$[36]	Volume, Å^3	405.84	424.25	411.29
(P -1)	a, Å	6.42	6.47	6.49
	b, Å	7.76	7.88	7.84
	c, Å	8.59	8.67	8.51
	α,^{o}	91.66	92.09	92.10
	β,^{o}	105.37	104.83	104.80
	γ,^{o}	99.39	99.56	99.50
$LiBO_2$[33]	Volume,Å^3	119.79	116.23	114.64
(I-$42d$)	a, Å	4.22	4.16	4.20
	c, Å	6.74	6.73	6.51
Li_3BO_3[32]	Volume, Å^3	276.80	242.66	244.59
($P1\ 2_1/c\ 1$)	a, Å	3.39	3.26	3.27
	b, Å	9.65	9.21	9.18
	c, Å	8.62	8.23	8.32
	β,^{o}	100.69	101.06	101.10

* was used for creating of B_1-O-B_1 interaction

have been reoptimized in order to obtain charge neutrality. The atomic charges of $Li_2B_4O_7$ (Tab. 1) would lead to charged unit cells for the other stoichiometries. Since the Li ion has different oxygen environments in different crystals, it is necessary to change its charge by using the expression $q_{\mathrm{Li}} = -\left(n_{\mathrm{O}} \cdot q_{\mathrm{O}} + n_{\mathrm{B}^1} \cdot q_{\mathrm{B}^1} + n_{\mathrm{B}^2} \cdot q_{\mathrm{B}^2}\right)/n_{\mathrm{Li}}$. Here n_{Li}, n_{O}, n_{B^1} and n_{B^2} are the number of Li, O, B^1 and B^2 ions, respectively. q_{O}, q_{B^1} and q_{B^1} are the charges of the O, B^1, B^2 ions (taken from Tab. 2). The modification of the charges for different crystals is not new. In a previous study the potential model for $(Li_2O)_x(B_2O_3)_{1-x}$ ($x = 0 \div 0.4$) was also based on different charges of the B and O atoms [24]. In that study the charge of Li atom was set to +1.

The results obtained with the present approach are in good agreement with experimental data. The maximal deviation between calculated and experimental values of the lattice parameters is found for the LiB_3O_5 crystal (0.45 Å for a). In general the error of lattice vectors is smaller than 0.25 Å and 0.6 degrees for angles. These are errors in a range typical for empirical calculations.

However, the calculation of other crystal properties gave partly nonphysical results, namely negative values of the acoustic modes at the Γ point. Therefore we assumed that not only the q_{Li} had to be changed but also the q_{O}. We fitted the Li and O charges in equation (2) to the crystallographic crystal data and to the values of the acoustic modes at the Γ point, which are equal to zero. The other parameters of the potentials (1) and (2) were kept constant. This procedure of fitting of the charges to the lattice parameters opens the possibility to create a potential model which can predict not only lattice parameters of single crystals of the Li_2O-B_2O_3 system, but the phonon properties too. The new charges are listed in Table 4. Significant improvement for the lattice vectors (see Tab. 1) was obtained for Li_3BO_3 (the error of vector b was reduced from 0.47 Å to 0.03 Å) and for LiB_3O_5 (for vector a the deviation of 0.45 Å became 0.03 Å). For the other crystals small changes of the structure parameters were obtained compared to those shown in Table 1.

Table 4. Adjusted effective charges for the crystals Li_2O-B_2O_3 system.

Element	Li_3BO_3	$LiBO_2$	$Li_2B_4O_7$	$Li_3B_7O_{12}$	LiB_3O_5
Li	0.596	0.671	0.664	0.646	0.607
B^1	1.072	1.072	1.072	1.072	1.072
B^2	-	-	1.223	1.223	1.223
O	−0.953	−0.871	−0.846	−0.825	−0.795

The fitted O charges plotted as a function of the mole fraction of Li_2O give an almost straight line (see Fig. 3). The maximum deviation from the linear curve is ±0.02.

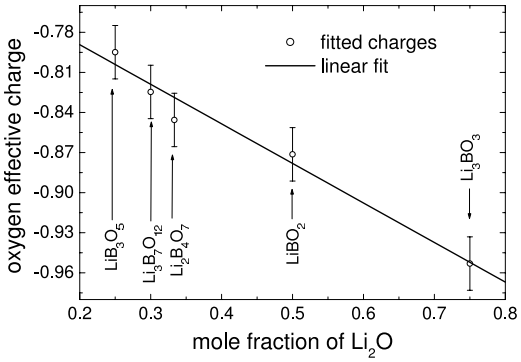

Fig. 3. Oxygen charge dependence on the mole fraction of Li_2O.

It is obvious also from Table 4 that there must be a correlation between q_O and q_{Li}, which expresses qualitatively the charge transfer between the different ions. The decrease of the effective charges q_O with increasing Li_2O mole fraction is a result of the different oxygen coordination of the lithium atoms, which change from 8 (for $LiBO_2$) to 5 (for LiB_3O_5). The exception is only Li_3BO_3, where the oxygen atoms do not connect two BO_n ($n = 3$ or 4) units and, in turn, interact more with the Li atoms than in the other crystals of the Li_2O-B_2O_3 system. Therefore, the charges q_O and q_{Li} in Li_3BO_3 are smaller.

The dependence of O charges on the mole fraction of Li_2O can be used to extend the range of application of the potential model to other crystals of the Li_2O-B_2O_3 system. The obtained results for the lattice parameters agree well with experiment, and give a better description than results without fitting the oxygen and lithium charges (Tab. 3). The error of lattice vectors does not exceed 0.22 Å (largest error obtained for a_{LiBO_2}) and 0.06 degree for angles.

4 Summary and conclusions

A classical model is proposed for the description of crystalline solids in Li_2O-B_2O_3 systems. Two types of B atoms are distinguished based on their coordination, B^1 and B^2, that are the part of BO_3 and BO_4 subunits of the lattice, respectively. Ab initio calculations of the properties of the principal crystal structural complexes, i.e. the BO_3 triangle and the BO_4 tetrahedron, revealed the need to describe these two boron atoms with different parameter sets. On this basis an effective classical potential model was obtained. The analysis of the behavior of the boron-oxygen interatomic potentials showed the pronounced difference between both functions. We conclude, that for borate crystals it is essential to take into account the non-equivalence of boron atoms in BO_3 and BO_4. Also for other systems, where both sp^2 and sp^3 hybridizations of the same element are present, it may be necessary to take this into account.

The potential model was used to calculate structural parameters for Li_3BO_3, $Li_6B_4O_9$, $LiBO_2$, $Li_2B_4O_7$, LiB_3O_5 and $Li_3B_7O_{12}$ crystals. The obtained results are in good agreement with experimental data. We tested by molecular dynamics calculations that it is not necessary to take into account changes of the boron atoms environment for temperatures below 900 K. Our potential model also enable us to calculate phonon spectra and to model the abnormal temperature dependence of lattice parameters of $Li_2B_4O_7$ and LiB_3O_5 successfully. These results will be described in forthcoming publications.

An analysis of the Li environment gives a linear dependence of oxygen charges on the molar fraction of Li_2O. This interpolation allows to apply the present potential model also to other crystals of the Li_2O-B_2O_3 systems.

Based on our results, we assume that the suggested approach allows to determine different properties of crystalline and vitreous solids of Li_2O-B_2O_3 systems. Moreover it can be useful for other crystals based on the boron-oxygen anion subsystem.

This work was supported by the Deutscher Akademischer Austausch Dienst. The author is grateful to Prof. V.M. Rizak for suggesting the subject of studies, to Dr. V.M. Holovey, Dr. K.Z. Rushchanskii for valuable comments and to Prof. Snigurskij O. for his help.

References

1. B.S.R. Sastry, F.A. Hummel, J. Am. Ceram. Soc. **41**, 7 (1958)
2. B.S.R. Sastry, F.A. Hummel, J. Am. Ceram. Soc. **42**, 216 (1959)
3. V.I. Aver'yanov, A.E. Kalmykov, Glass Phys. and Chemistry **16**, 492 (1990)
4. J. Huang, Y. Shen, Appl. Phys. Lett. **15**, 1579 (1991)
5. Mao Hongnei, Appl. Phys. Lett. **61**, 1148 (1992)
6. T. Ukachi, R.J. Lane, J. Opt. Soc. Amer. B. **9**, 1128 (1992)
7. F. Hanson, D. Dick, Opt. Lett. **16**, 205 (1991)
8. Y. Wang, Z. Xu, D. Deng et al., Appl. Phys. Lett. **55**, 7 (1989)
9. B. Wu, F. Xie, C.C.D. Deng, Z. Xu, Opt. Commun. **88**, 451454 (1992)
10. J. Hee-Rak, J. Byung-Moon, Ch. Jung-Won, K. Jung-Nam, Materials Letters. **30**, 41 (1997)
11. K. Otsuka, M. Funami, M. Ito et al., Jpn J. Appl. Phys. **34**, 2646 (1995)
12. M. Takeuchi, I. Odagawa, M. Tanaka, K. Yamanouchi, Jpn J. Appl. Phys. **36**, 3091 (1997)
13. K.V. Shestopalov, V.A. Nefedov, B.I. Zadneprovsky, *In.: Proc. 1994 IEEE Int. Frequency Control Symp.*, 301 (Boston, USA, 1994)
14. M. Ono, M. Sakai, Y. Fujiwara, N. Wakatsuki, *In.: Proc. 1997 IEEE Ultrasonics Symp.* **2**, 1047 (Toronto, Canada, 1997)
15. R. Komatsu, T. Sugawara, K. Sassa et al., Appl. Phys. Lett. **70**, 3492 (1997)
16. C. Furetta, P.S. Weng, *Operation Thermoluminescent dosimetry* (World Scientific, London, 1998)
17. K. Mahesh, P.S. Weng, C. Furetta, *Thermoluminescence in solids and its applications* (Nuclear Technology Publishing, Ashford, 1989)

18. E.F. Dolzhenkova, V.N. Baumer, A.V. Tolmachev, B.M. Hunda, P.P. Puga, *6th Intern. Confer. on Inorganic Scintillators and their Applications* (Book of Abstracts, Chamonix, France, 2001), p. 210
19. G. Kanchan, A.J. Patkan, H.B. Lai, J. Mater. Sci. **23**, 4257 (1988)
20. A. Kirfel, G. Will, R.F. Stewart, Acta Crystallogr. B **39**, 175 (1983)
21. A. Takada, C.R.A. Catlow, G.D. Price, J. Phys.: Condens. Matter **7**, 8659 (1995); A. Takada, C.R.A. Catlow, G.D. Price, J. Phys.: Condens. Matter **7**, 8693 (1995)
22. R. Fernandez-Perea, F.J. Bermejo, M.L. Senent, Phys. Rev. B **54**, 6039 (1996)
23. H. Inoue, N. Aoki, I. Yasui, J. Am. Ceram. Soc. **70**, 622 (1987)
24. A.H. Verhoef, H.W. den Hartog, J. Non-Crystaline Solids **182**, 235 (1995)
25. C.P.E. Varsamis, A. Vegiri, E.I. Kamitsos, Condens. Matter Phys. **4**, 119 (2001)
26. C.P.E. Varsamis, A. Vegiri, E.I. Kamitsos, Phys. Rev. B **65**, 104203 (2002)
27. A. Vegiria, C.P.E. Varsamis, J. Chem. Phys. **120**, 7689 (2004)
28. Q. Xu, K. Kawamura, T. Yokokawa, J. Non-Crystaline Solids **104**, 261 (1988)
29. J.D. Gale, Philos. Mag. B **73**, 3 (1996); J.D. Gale, J. Chem. Soc. Faraday Trans. **93**, 629 (1997); J.D. Gale, A.L. Rohl, Molec. Simulation **29**, 291 (2003)
30. G.E. Gurr, P.W. Montgomery, C.D. Knutson, B.T. Gorres, Acta Cryst. B: Struct. Sci. **26**, 906 (1970)
31. C.T. Prewitt, R.D. Shannon, Acta Cryst. B: Struct. Sci. **24**, 869 (1968)
32. F. Stewner, Acta Crystallogr. B **27**, 904 (1971)
33. M. Marezio, J.P. Remeika, J. Chem. Phys. **44**, 3348 (1966)
34. S.F. Radaev, L.A. Muradyan, L.F. Malakhova, Y.A. Burak, V.I. Simonov, Kristallografiya **34**, 1400 (1989)
35. S.F. Radaev, B.A. Maximov, V.I. Simonov, B.V. Andreev, V.A. D'yakov, Acta Crystallogr. B **48**, 154 (1992)
36. J. Aidong, L. Shirong, H. Qingzhen, C. Tianbin, K. Deming, Acta Crystallogr. C **46**, 1999 (1990)
37. P.P. Ewald, Ann. Phys. **64**, 253 (1921)
38. V.V. Zareckyj, Ya.V. Burac, Phys. of Solid State **31**, 80 (1989)
39. L. Bohaty, S. Haussuhl, J. Liebertz, Cryst. Res. Technol. **24**, 1159 (1989)
40. J.D. Dill, J.A. Pople, J. Chem. Phys. **62**, 2921 (1975)
41. V.R. Saunders, R. Dovesi, C. Roetti et al., *CRYSTAL2003 User's Manual* (University of Torino, Torino, 2003)
42. C.N. Sokolov, I.N. Silin, *Preprint JINR, D-810* (Dubna, 1961)
43. I.N. Silin, *FORTRAN program library* (Dubna, JINR, D-520, 1970)
44. R.S. Mulliken, J. Chem. Phys. **23**, 2343 (1982)
45. W.H. Press, S.A. Teukolsky, W.T Vetterling B.P. Flannery, *Numerical Recipes*, 2nd edn. (Cambridge University Press, Cambridge, 1992)
46. A.V. Vdovin, V.N. Moiseenko, V.S. Gorelik, Ya.V. Burak, Phys. Sol. State **43**, 1648 (2001)
47. A. Takada, C.R.A. Catlow et al., Phys. Rev. B **51**, 1447 (1995)
48. H.A.A. Sidek, G.A. Saunders, B. James, J. Phys. Chem. Solids. **51**, 457 (1990)
49. M. Adachi, T. Shiosaki et al., *IEEE Ultrason. Symp. Proc.* (San Francisco, Calif.), **1**, 228 (1985)
50. W.G. Hoover, Phys. Rev. A **31**, 1695 (1985)
51. M. Parrinello, A. Rahman, J. Appl. Phys. **52**, 7182 (1981)